ASTROBIOLOGY
Volume 22, Number 10, 2022

DOI: 10.1089/ast.2022.0013

Mars-like UV Flux and Ionizing Radiation Differently Affect Biomarker Detectability in the Desert Cyanobacterium *Chroococcidiopsis* as Revealed by the Life Detector Chip Antibody Microarray

Daniela Billi,[1] Yolanda Blanco,[2] Andrea Ianneo,[1] Mercedes Moreno-Paz,[2] Jacobo Aguirre,[2] Mickael Baqué,[3] Ralf Moeller,[4] Jean-Pierre de Vera,[5] and Victor Parro[2]

Abstract

The effect of a Mars-like UV flux and γ-radiation on the detectability of biomarkers in dried cells of *Chroococcidiopsis* sp. CCMEE 029 was investigated using a fluorescence sandwich microarray immunoassay. The production of anti-*Chroococcidiopsis* antibodies allowed the immunoidentification of a reduced, though still detectable, signal in dried cells mixed with phyllosilicatic and sulfatic Mars regolith simulants after exposure to 6.8×10^5 kJ/m^2 of a Mars-like UV flux. No signal was detected in dried cells that were not mixed with minerals after 1.4×10^5 kJ/m^2. For γ-radiation (^{60}Co), no detectable variations of the fluorescence signal occurred in dried cells exposed to 113 kGy compared to non-irradiated dried cells. Our results suggest that immunoassay-based techniques could be used to detect life tracers eventually present in the martian subsurface in freshly excavated materials only if shielded from solar UV. The high structural integrity of biomarkers irradiated with γ-radiation that mimics a dose accumulated in 13 Myr at 2 m depth from the martian surface has implications for the potential detectability of similar organic molecules/compounds by future life-detection missions such as the ExoMars Rosalind Franklin rover. Key Words: Biomarkers—Life detector—Cyanobacteria—Mars-like UV—Ionizing radiation. Astrobiology 22, 1199–1209.

1. Introduction

The detection of biosignatures in the Solar System is one of the great challenges of current and upcoming *in situ* robotic missions and future space missions once the return of samples to Earth is technically feasible (Martins, 2020). Current life-detection technologies are based on miniaturized mass spectrometry and Raman spectroscopy (Marshall *et al.,* 2010; Arevalo *et al.,* 2020), and indeed, the NASA Perseverance and the ESA Rosalind Franklin rovers are equipped to perform Raman spectroscopic measurements of martian subsurface samples (Rull *et al.,* 2017; Wiens *et al.,* 2021). Other promising techniques are under development based on nanopore sequencing for detecting nucleic acid–based life (Carr *et al.,* 2020; Maggiori *et al.,* 2020), while an antibody-based technique, known as the Signs of Life Detector (SOLID)-LDChip system, has already been developed for *in situ* biomarker detection (de Diego-Castilla *et al.,* 2011; Parro *et al.,* 2011). A bioaffinity-based system was recently included together with Raman spectroscopy and microscopic techniques into a novel instrument suite named Complex Molecules Detector (CMOLD), which could constitute a scientific payload in future planetary exploration (Fairén *et al.,* 2020). The LDChip system was successfully

[1]University of Rome Tor Vergata, Department of Biology, Rome, Italy.
[2]Centro de Astrobiología (CAB), CSIC-INTA, Department of Molecular Evolution, Torrejón de Ardoz, Madrid, Spain.
[3]German Aerospace Center (DLR), Institute of Planetary Research, Planetary Laboratories Department, Berlin, Germany.
[4]German Aerospace Center (DLR), Institute of Aerospace Medicine, Radiation Biology Department, Cologne, Germany.
[5]German Aerospace Center (DLR), Space Operations and Astronaut Training, Microgravity User Support Center, Cologne, Germany.

used to detect microbial biomarkers from multiple extreme, anaerobic, and salty Mars analog fields (*e.g.,* Rivas *et al.,* 2008; Parro *et al.,* 2011; García-Descalzo *et al.,* 2019; Sánchez-García *et al.,* 2020) in the presence of perchlorate concentrations 20 times higher than that found on Mars (Parro *et al.,* 2011).

Indeed, Mars analog fields are a reservoir of microorganisms used as models for understanding long-term survival and biomarker stability in habitable surface/subsurface environments on Mars (Martins *et al.,* 2017). On Earth, due to the low temperature and extreme liquid water scarcity, the Dry Valleys in Antarctica and the Atacama Desert in Chile are considered the closest hyper-arid analogs of Mars (Cassaro *et al.,* 2021; Azua-Bustos *et al.,* 2022). Since on Earth the transition from arid to hyper-arid deserts causes a shift from edaphic communities to lithic communities and finally to communities in hygroscopic substrates, it is conceivable that, if life occurred on Mars, it may have withdrawn to subsurface environments (Davila and Schulze-Makuch, 2016).

Cyanobacteria of the genus *Chroococcidiopsis* that take refuge within or under rocks in the most extreme hot and cold desert environments are a model organism for searching traces of life on Mars (Friedmann and Ocampo, 1976). Although there is no general agreement as to whether photosynthesis ever occurred on Mars (Cockell and Raven, 2004; Westall *et al.,* 2015), the presence of cyanobacteria capable of far-red photosynthesis in Earth's caves (Behrendt *et al.,* 2020) raises the possibility of phototrophic microorganisms in martian caves (Azua-Bustos *et al.,* 2022). Notably, far-red shifted photosynthetic pigments were detected in *Chroococcidiopsis* cells in hypolithic rocks from the Mojave Desert (Smith *et al.,* 2014).

The martian surface is essentially sterilized by solar UV radiation (Cockell *et al.,* 2000). In the laboratory, a dried monolayer of *Chroococcidiopsis* sp. 029 was eradicated by a 30 min exposure to a simulated Mars-like UV flux, although survivors were scored under 1 mm rock fragments (Cockell *et al.,* 2005). The detrimental effect of an unattenuated Mars-like UV flux on cyanobacterial pigment autofluorescence and Raman signal was reported during the EXPOSE-E space mission, which was performed using the ESA facility installed outside the International Space Station (Cockell *et al.,* 2011). The protective role of regolith was reported for dried cells of *Chroococcidiopsis* sp. 029 that were mixed with martian soil simulants and exposed during the Biology and Mars Experiment (BIOMEX) space experiment to UV radiation corresponding to 4 h on the martian surface (Billi *et al.,* 2019).

The ionizing radiation dose that reaches the martian surface (about 76 mGy/year; Hassler *et al.,* 2014) is not lethal to the majority of terrestrial microorganisms, especially those that are radioresistant, such as *Chroococcidiopsis* sp. 029, and capable of tolerating up to 24 kGy of γ-rays in the hydrated state (Verseux *et al.,* 2017). However, in near-surface frozen habitats on Mars, a putative dormant life would accumulate high doses of cosmic rays over geological timescales and eventually be eradicated (Dartnell *et al.,* 2007). In this scenario, the endurance of dried *Chroococcidiopsis* after exposure to 2 kGy of Fe-ion radiation further expanded our appreciation of the resilience of a putative dormant life in the martian subsurface (Mosca *et al.,* 2022). Remarkably, a strong Raman carotenoid signal was still detectable in dried cells of *Chroococcidiopsis* sp. 029 irradiated with 113 kGy of γ-rays (Baqué *et al.,* 2020), a dose accumulated in about 1.5 Myr on the martian surface and in 13 Myr at 2 m depth (Hassler *et al.,* 2014).

In the present study, we tested the biomarker detectability in dried *Chroococcidiopsis* cells exposed to Mars-like UV flux and γ-rays using the LDChip multiplex fluorescence immunoassay system. Since this antibody-based technique will give a positive response if an antibody binds the corresponding antigen that has preserved an intact or slightly modified epitope (Blanco *et al.,* 2018), we first verified whether suitable antibodies could be obtained from *Chroococcidiopsis* cells and whether they could bind low antigen levels. Then, we evaluated the immunoidentification signals in dried cells mixed and cells not mixed with martian soil simulants after exposure to up to 6.8×10^5 kJ/m^2 of a Mars-like UV flux and irradiation with 113 kGy of γ-rays.

2. Material and Methods

2.1. Strains and culture conditions

Chroococcidiopsis sp. CCMEE 029 and CCMEE 057 were isolated by Roseli-Ocampo Friedmann from endolithic communities in sandstone from the Negev Desert (Israel) and in granite from the Sinai Desert (Egypt), respectively. These strains are currently kept in the Laboratory of Astrobiology and Molecular Biology of Cyanobacteria, Department of Biology, University of Rome Tor Vergata, as part of the Culture Collection of Microorganisms from Extreme Environments (CCMEE) established by E. Imre Friedmann. Cyanobacteria were grown under routine conditions at 25°C in BG-11 medium under a photon flux density of 40 μmol/m^{2}s^1 provided by fluorescent cool-white bulbs with a 16/8 h light/dark cycle.

2.2. Exposure to Mars-like UV flux

Aliquots of about 2×10^9 cells of *Chroococcidiopsis* sp. CCMEE 029 were obtained from 2-month-old liquid cultures and pellets plated with 2 g of Phyllosilicatic Mars Regolith Simulant (P-MRS) or Sulfatic Mars Regolith Simulant (S-MRS) in a 100 mm diameter Petri dish on top of BG-11 agarized medium. P-MRS is a mixture of montmorillonite (45%), Fe_2O_3, chamosite, kaolinite, siderite, hydromagnesite, quartz, gabbro, and dunite that simulates the acid regolith cover from early evolutionary stages of Mars; S-MRS contains gypsum (30%), hematite, goethite, quartz, gabbro, and dunite, which mimics the basic regolith cover from late Mars (de Vera *et al.,* 2019). Controls were performed by plating cyanobacterial pellets without minerals on top of BG-11 agarized medium (hereinafter referred to as no-mineral control). Samples were air-dried overnight in a sterile hood with disks cut to the size of the exposure carrier cells (~ 115 mm^2) under sterile conditions.

Dried samples were exposed to EVT2 (Environmental Verification Tests part 2), which was performed in the frame of the BIOMEX project at the Planetary and Space Simulation facilities (DLR, Institute of Aerospace Medicine, Cologne, Germany), as previously described (de Vera *et al.,* 2019). Samples were exposed to a polychromatic UV (200–400 nm) radiation produced by a solar simulator SOL2000

at 1271 W/m^2. Samples were continuously cooled by a temperature-controlled copper interface part of the PSI facility to keep temperatures below 25°C (average measured temperature 22 ± 1°C). EVT tests were performed in triplicate, and controls were kept at the German Aerospace Center (DLR) in the dark at room temperature. The final doses are reported in Table 1.

2.3. Exposure to γ-radiation

Samples that contained about 1.5×10^8 cells of *Chroococcidiopsis* sp. CCMEE 029 were obtained from cultures in the early stationary phase, filtered on Millipore filters, and then air-dried overnight in a sterile hood. Samples were irradiated with γ-radiation in the context of the STARLIFE project using a C-188 cobalt-60 source provided by Beta-Gamma-Service (Cologne, Germany), with a dose rate of 100 Gy/min, at room temperature as previously described (Verseux *et al.,* 2017). The final doses are reported in Table 1.

2.4. Production of antibodies to Chroococcidiopsis strains and microarray production

Rabbit polyclonal antibodies were produced to *Chroococcidiopsis* sp. CCMEE 029 and CCMEE 057, both with biomass from liquid BG-11 cultures (K19, K21) and from several-months-grown biomass on solid BG-11 (K18, K20), respectively, as described previously (Rivas *et al.,* 2008). We used a variety of different culture media and conditions because it was likely for different antigens to be associated with different growth modalities, for example, planktonic in a flask versus biofilm-like on solid support. The IgG fraction (protein A-purified) of each antibody, together with 17 additional antibodies to other planktonic and benthic cyanobacterial strains (Blanco *et al.,* 2015), was printed on a triplicate spot pattern (Fig. 1) in 3 × 8 identical microarrays per epoxy-activated microscope slide (Arrayit, CA, USA), so that up to 24 assays could be run simultaneously.

2.5. Fluorescent sandwich microarray immunoassay

The antibodies K18–K21 were titrated to determine their working concentration, sensitivity, specificity, and detection limit. For this, 50 μL of the corresponding immunogen (*i.e.,* partially ultrasonicated cell extract in 1X PBS injected to rabbit) and dilutions of it in PBST (1X PBS pH 7.4 and 0.1% Tween 20) were used as described previously (Blanco *et al.,* 2015). Cells exposed to Mars-like UV flux and γ-radiation, along with their respective controls, that is, no-mineral controls and non-irradiated cells, were resuspended in 2 mL of TBSTRR (0.4 M Tris-HCl pH 8, 0.3 M NaCl, and 0.1% Tween 20) to a final concentration of about 1×10^6 cells/mL (for UV-exposed cells) and 7.5×10^7 cells/mL (for γ-radiation exposed cells). After that, cells were sonicated for 5 cycles of 30 s and filtered through a 20 μm filter to prepare the extracts to be analyzed by fluorescent sandwich microarray immunoassay (FSMI) by using slides blocked with BSA and dried as described (Blanco *et al.,* 2015). Fifty microliters of the filtrate was directly incubated with the antibody microarray for 1 h at ambient temperature, washed three times with 150 μL of TBSTRR, and incubated again for 1 h with 50 μL of an Alexa 647-labeled antibody mixture containing the 4 anti-cyanobacterial strain antibodies. The concentration of each fluorescent antibody in the mixture ranged from 0.7 to 2 μg/mL. Slides were washed again, dried (as already described), and scanned for fluorescence at 635 nm in a GenePix 4100A scanner (Genomic Solutions, MI, USA). Blank controls using only buffer were

Table 1. Polychromatic UV and Gamma-Ray Radiation During the BIOMEX and STARLIFE Projects

Project name	*BIOMEX*		
Type of irradiation	*Polychromatic UV 200–400 nm (kJ/m^2)*	*Exposure time*	*Equivalent exposure time on Mars (days)*[a]
Intensity	0	0	0
	1.4×10^3	18 min	1
	1.4×10^4	3 h	9
	1.4×10^5	30 h	94
	4.5×10^5	99 h	303
	6.8×10^5	148 h	457

Project name	*STARLIFE*			
Type of irradiation	*Gamma irradiation (kGy)*	*Exposure time*	*Equivalent exposure time at Mars' surface (years)*[b]	*Equivalent exposure time 2 m below Mars' surface (years)*[b]
Intensity	0	0	0	0
	6.21	1 h	8.17×10^4	7.14×10^5
	11.59	2 h	1.53×10^5	1.33×10^6
	17.51	3 h	2.30×10^5	2.01×10^6
	23.92	4 h	3.15×10^5	2.75×10^6
	46.88	7 h 50 min	6.17×10^5	5.39×10^6
	72.16	12 h	9.49×10^5	8.29×10^6
	113.25	18 h 50 min	1.49×10^6	1.30×10^7

[a]Based on Cockell *et al.* (2000) and measurements from Mars Science Laboratory (Gómez-Elvira *et al.,* 2014) for an average flux of 17 W/m^2.
[b]Based on the measurements by Mars Science Laboratory (Farley *et al.,* 2014; Hassler *et al.,* 2014).

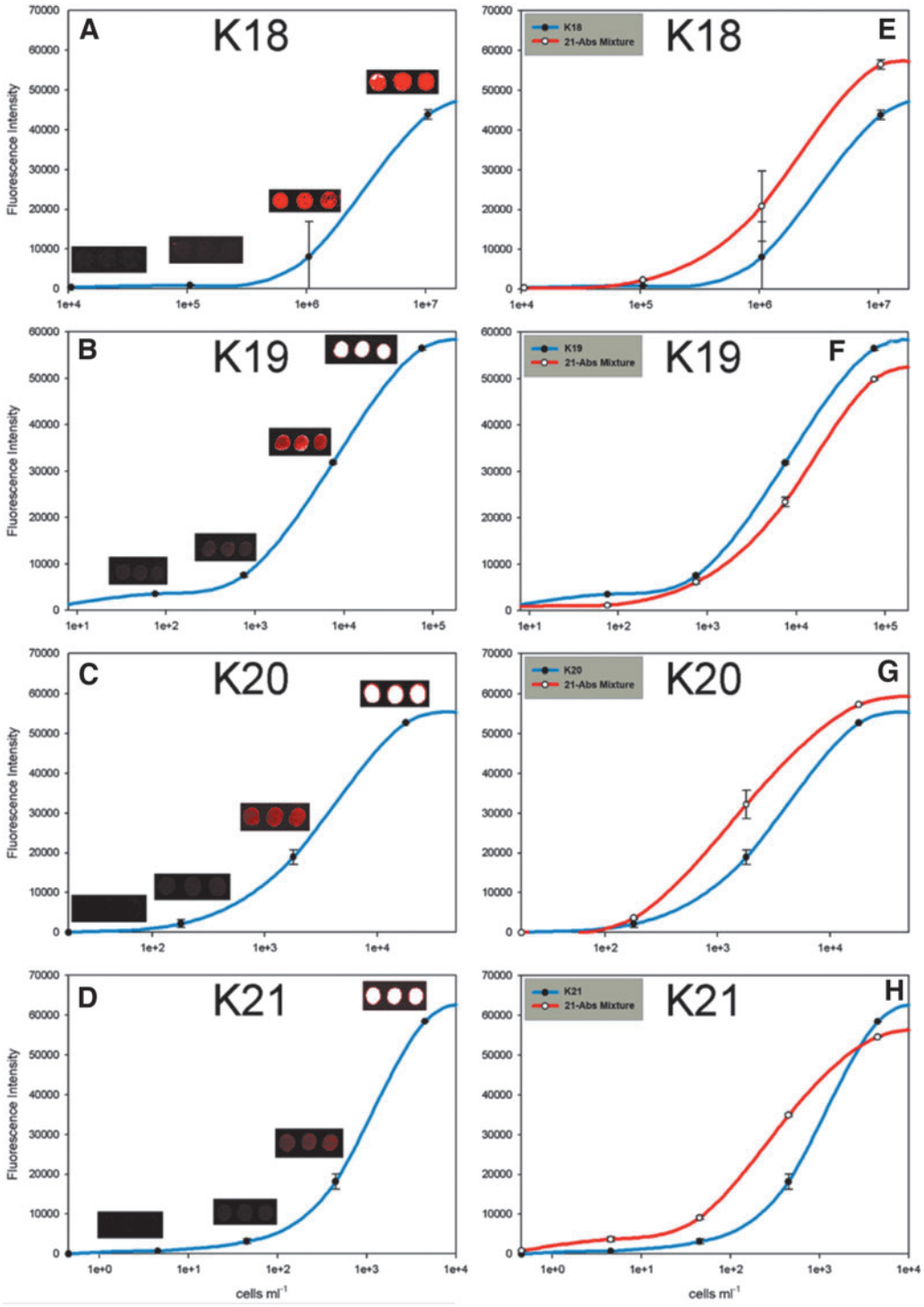

FIG. 1. Detection limits of antibodies to *Chroococcidiopsis* sp. CCMEE 029 (K18–K19) and to *Chroococcidiopsis* sp. CCMEE 057 (K20–K21). Calibration curves using different concentrations of cyanobacterial lysate (*i.e.,* immunogen) as antigen and fluorescent antibody at its working concentration (**A**–**D**) or fluorescent mixtures containing 21 anti-cyanobacterial antibodies (**E**–**H**). Detection of lysate of strain CCMEE 029 with fluorescent antibodies K18 and K19, respectively (A and B), and lysate of strain CCMEE 057 and fluorescent antibodies K20 and K21 (C and D), respectively. Detection of lysate of strain CCMEE 029 and the fluorescent mixture (red line in E and F) and lysate of strain CCMEE 057 and the fluorescent mixture (red line in G and H). For each experimental point of the curves, the original scanned image of the fluorescent spots in the microarray is shown.

run in parallel. The images were analyzed and quantified with GenePix Pro (Genomic Solutions, MI, USA). Fluorescence intensity A of each antibody spot was calculated using Equation 1:

$$A = (\text{F635} - B)_{\text{sample}} - (\text{F635} - B)_{\text{blank}} \quad (1)$$

where (F635 – B) is the fluorescence intensity at 635 nm minus the local background around the spots. An additional cutoff threshold of 1.5-fold, which was the average of the fluorescence intensity of the whole array, was applied to minimize the probability of false positives (Blanco *et al.,* 2015).

3. Results

3.1. Sensitivity of anti-Chroococcidiopsis antibodies

The detection limit of antibodies K18–K19 to *Chroococcidiopsis* sp. CCMEE 029 and K20–K21 to *Chroococcidiopsis* sp. CCMEE 057, obtained from cells grown in liquid (K19, K21) and on solid substrates (K18, K20), was determined by using serial dilutions of the corresponding immunogen or cyanobacterial lysate as antigen and the working concentration of each antibody as fluorescent tracer. The sensitivity for each antibody was also determined by incubating the antigen with a fluorescent mixture of 21 anti-cyanobacterial strain antibodies spotted onto the microarray, among which 17 corresponded to CYANOCHIP (Blanco *et al.,* 2015) plus antibodies K18–K21. When the immunoassays for which serial dilutions of cyanobacterial lysates were used as antigen and revealed with their corresponding antibodies, a detection limit of $\geq 10^2$ cells/mL was obtained for antibody K19, while a detection limit of $>10^5$ cells/mL was obtained for the K18 antibody. This low detection signal was likely due to a reduced rabbit immunization (Fig. 1A, 1B). For comparative purposes, the sensitivity of the two antibodies to *Chroococcidiopsis* sp. CCMEE 057, namely, K20 and K21, was likewise determined (Fig. 1C, 1D). A detection limit of $\geq 10^2$ cells/mL was obtained for the K21 antibody, while a detection limit between 10^2 and 10^3 cells/mL was determined for the K20 antibody (Fig. 1C, 1D).

When the limit of detection for the four antibodies was assayed by multiplex FSMI using a fluorescent mixture that contained the 21-anti-cyanobacterial antibodies spotted in the microarray as tracer, the limit of detection values for K18, K19, K20, and K21 decreased, which resulted in a higher sensitivity of their corresponding antigens (Fig. 1E–1H).

3.2. Specificity of anti-Chroococcidiopsis antibodies

The specificity of K18–K21 antibodies was tested, one by one, by FSMI, using each cyanobacterial lysate with its own fluorescent antibody as tracer as described (Blanco *et al.,* 2015). After analyzing the images, the fluorescence intensities were quantified and expressed as an antibody graph associated with the whole antibody microarray (Fig. 2). The mathematical method for deconvoluting antibody cross-reactivity in the FSMI is based on the estimation of the fluorescence intensity of one antibody spot on the microarray as the sum of all the antibodies that cross-react with it. This procedure is explained in detail in the work of Rivas *et al.* (2008).

As expected, K18, K19, K20, and K21 antibodies presented a complex network of cross-reactions among them, due to the high level of similarity between the two *Chroococcidiopsis* strains from which they were produced, but none of them showed cross-reactivity events with other cyanobacteria included in CYANOCHIP (Blanco *et al.,* 2015) (Fig. 2).

To study the potentiality of bioaffinity-based sensors in the detection of preserved biomarkers on the surface of Mars, FSMIs were performed by using cell lysates obtained from *Chroococcidiopsis* sp. CCMEE 029 exposed to Mars-like UV flux and γ-rays, the four anti-*Chroococcidiopsis* antibodies capturers (spotted onto the slide), and the same fluorescent antibodies as tracers. As schematized in Fig. 3, the rationale was that an antibody binds its corresponding antigen (epitope) only if it has intact or slightly modified epitopes, while the radiation exposure modifies the epitope structure making it unrecognizable by the corresponding antibody (Blanco *et al.,* 2018).

3.3. Effect of Mars-like UV flux on immunoidentification

The effect of a Mars-like flux on the immunoidentification of dried cells of *Chroococcidiopsis* sp. CCMEE 029 was evaluated by using the four anti-*Chroococcidiopsis* antibodies (Fig. 4). Results show that the increase of the Mars-like flux up to 6.8×10^5 kJ/m^2 was paralleled by an increasing loss of the immunoidentification signal, that is, loss of fluorescence after the multiplex FSMI by using antibodies K18 and K19 to CCMEE 029, and antibodies K20 and K21 to *Chroococcidiopsis* sp. CCMEE 057 (Fig. 4). A marked loss of the immunoidentification signal to undetectable values after 1.4×10^5 kJ/m^2 occurred in dried cells not mixed with minerals, that is, no-mineral control (Fig. 4). Dried cells mixed with P-MRS showed reduced immunoidentification signals to 21%, 18%, and 13% of their corresponding non-irradiated dried cells for K19, K20, and K21, respectively, after the highest UV dose (Fig. 4). While a strong signal occurred in dried cells mixed with P-MRS exposed to 6.8×10^5 kJ/m^2 for antibody K18, dried cells mixed with S-MRS exhibited detectable immunoidentification signals after UV irradiation, although of reduced intensities compared to cells mixed with P-MRS, except after 4.5×10^5 kJ/m^2 (Fig. 4).

3.4. Effect of γ-radiation on the immunoidentification

In the case of dried cells of *Chroococcidiopsis* sp. CCMEE 029 exposed to increasing doses of γ-rays up to 113 kGy, the visual analysis of the FSMI indicated no remarkable variations of the fluorescence signal with respect to non-irradiated control (Fig. 5A). The quantification of the fluorescence intensity resulted from the immunoassays after different radiation doses (6, 12, 18, 24, 47, 72, and 113 kGy) and that of control (0 kGy) showed a reduction of the signal intensity only after 47 kGy (Fig. 5B). Unlike antibodies K18 and K19 to CCMEE 029 and antibodies K20 and K21 to *Chroococcidiopsis* sp., CCMEE 057 showed high levels of fluorescence intensities after irradiation with the two highest doses (*i.e.,* 72 and 113 kGy) (Fig. 5B).

4. Discussion

In the present study, the LDChip system was tested by assessing the biomarker detectability in dried cells of the

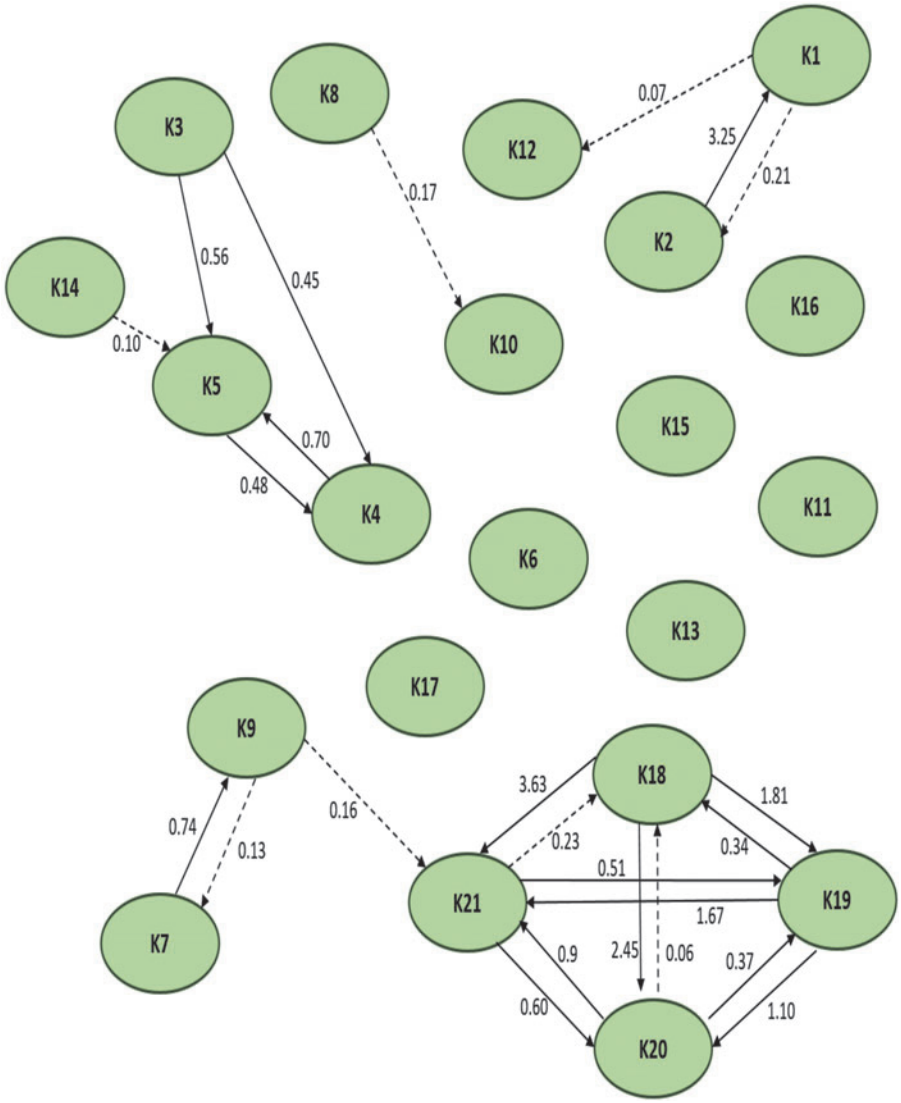

FIG. 2. Antibody graph G of 21 nodes and 24 links associated. Each node represents one antibody spotted on the microarray. The link (arrow) from antibody j to antibody i represents cross-reactivity of weight G_{ij}, where G_{ij} is the extent of cross-reactivity between antibodies i and j termed the cognate immunogen of antibody j (*i.e.*, weight $G_{ij}=1$ means the fluorescence signal obtained in the antibody spot when the FSMI is carried out using its immunogen/fluorescent antibody pair). Self-loops are not shown for the sake of clarity, and weak cross-reactivities ($G_{ij} < 0.25$) are printed in dashed lines. For further information, see Blanco *et al.* (2015).

cyanobacterium *Chroococcidiopsis* sp. CCMEE 029 exposed to Mars-like UV flux and ionizing radiation. Since this system is based on a fluorescence microarray immunoassay, four polyclonal antibodies to *Chroococcidiopsis* sp. CCMEE 029 (K18 and K19) and to *Chroococcidiopsis* sp. CCMEE 057 (K20 and K21) were produced and spotted on a microarray. The four antibodies showed a high level of sensitivity (about 10^2 cells/mL) except the antibody K18, likely due to a reduced rabbit immunization. Moreover, each antibody successfully detected immunogenic structures in dried *Chroococcidiopsis* cells mixed with martian regolith simulants and exposed to up to 6.8×10^5 kJ/m^2 of a Mars-like UV flux and in cells irradiated with γ-ray doses up to 113 kGy.

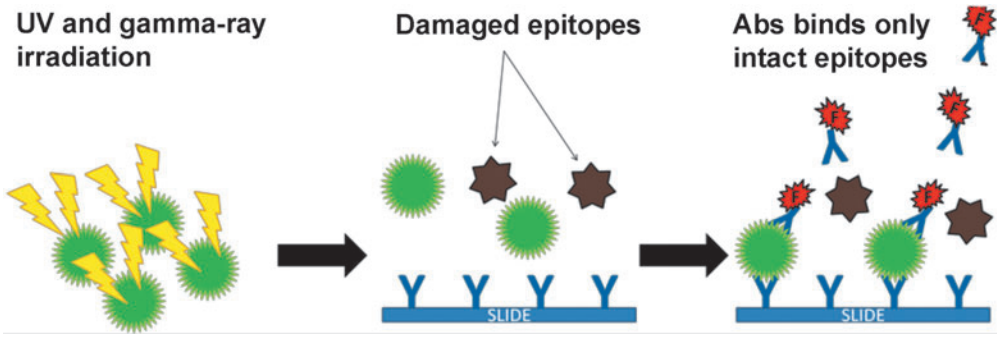

FIG. 3. Scheme of a FSMI showing intact or little modified epitopes (antigens) binding to immobilized corresponding antibodies and fluorescent antibodies (F); radiation-damaged epitopes do not bind the antibodies.

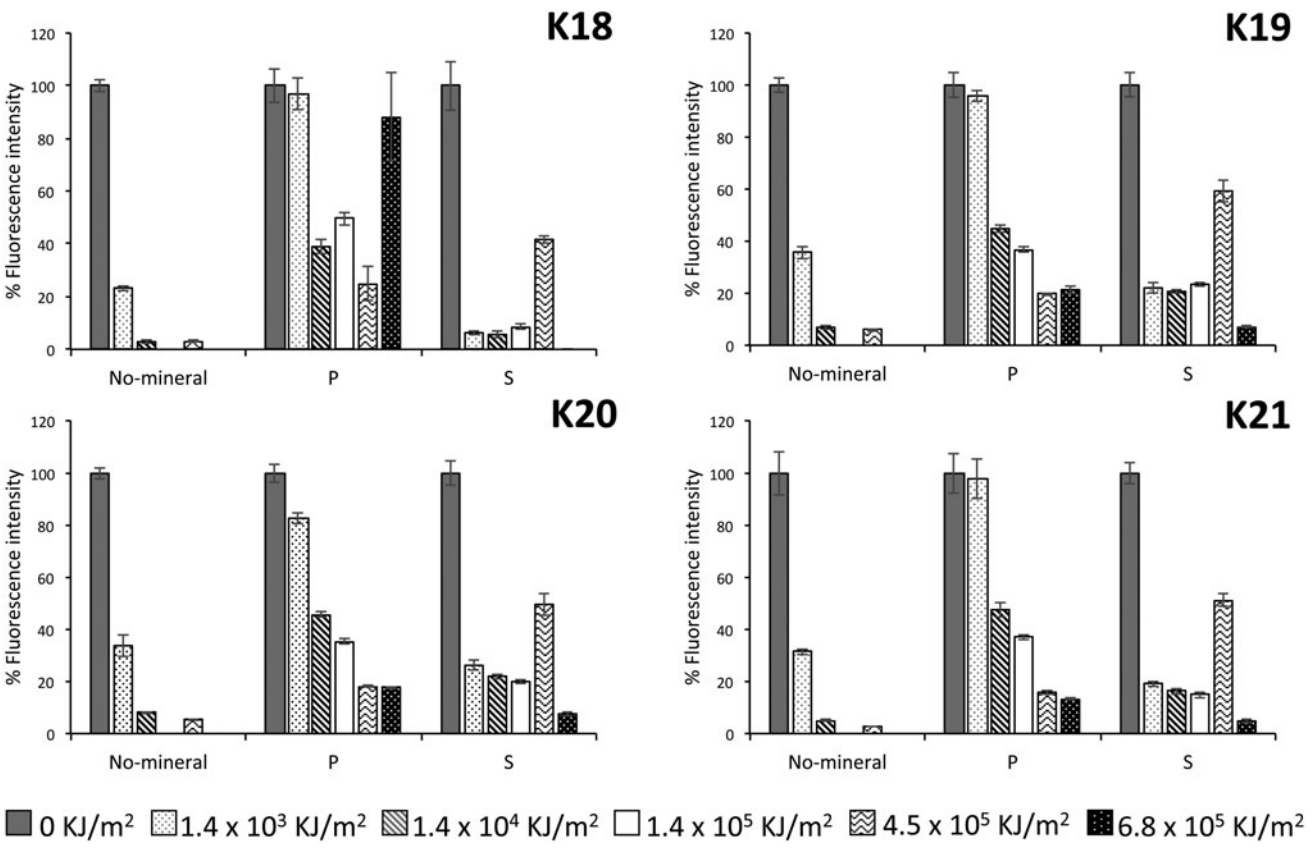

FIG. 4. Effect of a Mars-like UV flux on the immunoidentification of target compounds from *Chroococcidiopsis* sp. CCMEE 029 exposed to up to 6.8×10^5 kJ/m^2. The fluorescence intensity of the immunoassays of dried, irradiated cells was quantified and plotted as a function of non-irradiated dried cells, corresponding to 100%. No-mineral: irradiated, dried cells not mixed with minerals (control). S: irradiated, dried cells mixed with S-MRS. P: irradiated, dried cells mixed with P-MRS. The average intensities of six spots corresponding to each printed antibody (K18, K19, K20, and K21) are shown.

The UV radiation that reaches the martian surface causes a fast photodecomposition of organic compounds (Ertem *et al.,* 2017; Carrier *et al.,* 2019). A 1000 min exposure of sulfur-rich organics to a Mars-like UV flux reduced the Raman signal to 1/3, thus suggesting that freshly excavated S-rich organics could be detected only if shortly exposed to UV (Megevand *et al.,* 2021). However, 2 mm mineral coverings were reported to provide shielding against photodecomposition (Ertem *et al.,* 2017; Carrier *et al.,* 2019). Therefore, it is not surprising that the LDChip system did not detect any signal in dried *Chroococcidiopsis* cells exposed to Mars-like UV doses ranging from 1.4×10^3 kJ/m^2 to 6.8×10^5 kJ/m^2. While the detectable, although reduced, immunoidentification signal in *Chroococcidiopsis* cells mixed with P-MRS and S-MRS and exposed to up to 6.8×10^5 kJ/m^2 of UV radiation suggests that eventual mild changes induced in the antigen structures still allowed the interaction with each of the four antibodies, the higher immunoidentification signal detected in UV-irradiated *Chroococcidiopsis* cells mixed with P-MRS compared to S-MRS samples may have been due to the greater thickness of P-MRS samples (4–5 cell layers) as compared to S-MRS samples (2–3 cell layers), which was likely allowed by the P-MRS thinner grain-size (Baqué *et al.,* 2016). The opposite result scored in S-MRS samples irradiated with 4.5×10^5 kJ/m^2 might be ascribable to non-homogeneous association of cells with minerals (Baqué *et al.,* 2016).

Solar energetic particles and galactic cosmic radiation that reach the martian surface can penetrate down to 2 m depth (Hassler *et al.,* 2014), but with an energy flux of about 10^4 times less than UV photons, they destroy surface organics in longer timescales (hundreds of millions of years vs. days; Fox *et al.,* 2019). The irradiation with 113 kGy γ-rays of dried cells of *Chroococcidiopsis* sp. CCMEE 029 did not alter the structural integrity of epitopes that were detected by the LDChip system. This dose is accumulated in about 1.5 Myr on the martian surface and in 13 Myr at 2 m depth (Table 1), which results in extending the limit for immunoidentification recognition to timescales that exceed 13 Myr at 2 m depth below the martian surface. An accumulated dose of 10 Myr at 2 m below the martian surface was previously indicated as the immunoidentification limit for the fluorescence sandwich microarray immunoassay carried out on whole microorganisms (*Bacillus subtilis* spores), macromolecules (*e.g.,* proteins, bacterial exopolymeric substances and lipopolysaccharides), and small molecules (amino acids, monosaccharides, carboxylic acid derivatives, and peptides), although such an immunoidentification endpoint might not apply to all biomarkers (Blanco *et al.,* 2018).

The structural conformational integrity of epitopes in *Chroococcidiopsis* dried cells exposed to 113 kGy of γ-rays is likely due to its capability to efficiently stabilize subcellular components upon air-drying, a feature associated with oxidative stress avoidance upon desiccation (Fagliarone

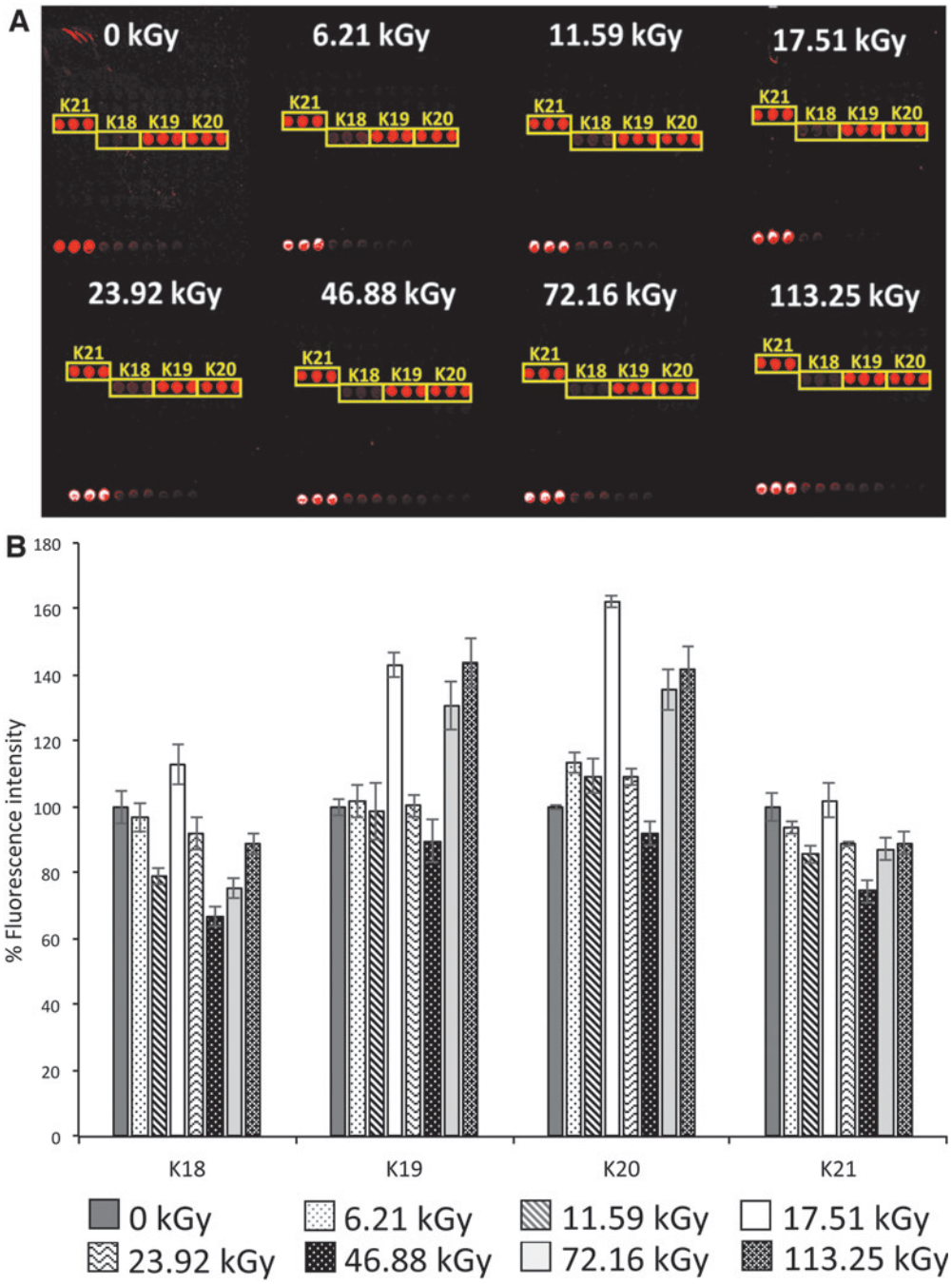

FIG. 5. Effect of ionizing radiation on immunoidentification of target compounds from cell lysates of *Chroococcidiopsis* sp. CCMEE 029 exposed to up 113.23 kGy of gamma rays. Fluorescent images of the spots on the microarray after FSMIs revealing the exposed cell lysates with the four anti-*Chroococcidiopsis* antibodies (**A**). Quantification of the fluorescence intensity of the FSMIs of dried irradiated and non-irradiated cells (0 kGy) (**B**). Fluorescence intensity was quantified and plotted as a function of non-irradiated cells corresponding to 100%. Data were calculated as the average of the intensities of three spots corresponding to each antibody on the microarray.

et al., 2017) and sucrose and trehalose accumulation (Fagliarone *et al.,* 2020). On the contrary, the Raman carotenoid signal was destroyed in dried cells of *Nostoc* sp. strain CCCryo 231-06 exposed to 27 kGy, but still detectable after 117 kGy of γ-rays in cells mixed with martian regolith simulants (Baqué *et al.,* 2018).

The effects of ionizing radiation also depend on exposure conditions. For instance, enzymatic activities were detected when irradiating with 100 kGy of γ-rays at low pressure and low temperature (Cheptsov *et al.,* 2021). In the absence of minerals, 37 kGy of γ-rays caused an 85% degradation of purine and uracil, whereas Ertem *et al.* (2021) observed 10% degradation under 5 cm of a martian soil simulant. Notably, the latter simulated the radiation dose accumulated in 500,000 years at a depth at which the Curiosity rover is currently collecting soil samples on Mars (Sunshine, 2010).

Moreover, the radiolytic degradation of soil organics from the Mojave Desert showed that levels <1 ppb should be reached on Mars in less than 1,700 Myr at 0.1 m depth and in 4,300 Myr at 1 m depth, so that the ExoMars Rosalind Franklin rover is likely to encounter pristine organics at ≥1.5 m depth (Vago *et al.,* 2017; Rojas Vivas *et al.,* 2021).

5. Conclusion

The detectability of immunoidentification signals in dried *Chroococcidiopsis* cells mixed with martian regolith simulants and exposed to Mars-like UV flux suggests that the Life Detector (SOLID)-LDChip system could be successfully used with freshly excavated materials shielded from solar UV. The absence of a significative reduction in the immunoidentification of targets in dried cells exposed to an ionizing radiation dose accumulated in 13 Myr at 2 m below the martian surface further supports the possibility of detecting traces of life at a depth that the ExoMars rover Rosalind Franklin will be sampling or even at 1 m depth as the IceBreaker mission concept proposed for martian permafrost (McKay *et al.,* 2013). Moreover, the biomarker detectability could be extended over geological timescales. In fact, the endurance of ancient permafrost samples irradiated with 40 kGy of γ-rays suggests cryoconservation of putative microbial communities for at least 8 Myr at 5 m below the martian surface (Cheptsov *et al.,* 2018). Therefore, such a survival potential over prolonged periods is relevant when considering that clement climate episodes might have occurred in the post-Noachian and allowed the revival and repair of radiation-accumulated damage in dormant microbial forms, hence resetting the survival clock (Hassler *et al.,* 2014) and extending biosignature detectability.

Authorship Contribution

D.B.: Conceptualization, writing original draft. Y.B.: Investigation, formal analysis; writing, review and editing. A.I.: Investigation. M.M.-P.: Investigation. J.A.: Formal analysis. M.B.: Review and editing. R.M.: resources, review and editing. J.-P. deV.: Resources, review and editing. V.P.: Conceptualization, supervision, resources, review and editing.

Funding

This research was supported by the Italian Space Agency, through the project BIOSIGN_Cyano (grant no. 2018-15-U.0 to D.B.) and grants no. ESP2015-69540-R, RTI2018-094368-B-I00 and MDM-2017-0737 Unidad de Excelencia ''Maria de Maeztu''-Centro de Astrobiología (INTA-CSIC), by the Spanish Ministry of Science and Innovation/State Agency of Research MCIN/AEI/10.13039/501100011033 and by ''ERDF A way of making Europe'' (to V.P.). R.M. was supported by the DLR grant FuE-Projekt ''ISS LIFE'' (Programm RF-FuW, Teilprogramm 475).

References

Arevalo R Jr, Ni Z, Danell RM. Mass spectrometry and planetary exploration: A brief review and future projection. *J Mass Spectrom* 2020;55(1):e4454; doi: 10.1002/jms.4454.

Azua-Bustos A, González-Silva C, Fairén AG. The Atacama Desert in Northern Chile as an analog model of Mars. *Front Astron Space Sci* 2022;8; doi: 10.3389/fspas.2021.810426.

Baqué M, Verseux C, Böttger U, *et al.* Preservation of biomarkers from cyanobacteria mixed with Mars-like regolith under simulated Martian atmosphere and UV flux. *Orig Life Evol Biosph* 2016;46(2–3):289–310; doi: 10.1007/s11084-015-9467-9.

Baqué M, Hanke F, Böttger U, *et al.* Protection of cyanobacterial carotenoids' Raman signatures by martian mineral analogues after high-dose gamma irradiation. *J Raman Spectrosc* 2018;49(10):1617–1627; doi: 10.1002/jrs.5449.

Baqué M, Napoli A, Fagliarone C, *et al.* Carotenoid Raman signatures are better preserved in dried cells of the desert cyanobacterium *Chroococcidiopsis* than in hydrated counterparts after high-dose gamma irradiation. *Life (Basel)* 2020; 10(6):83; doi: 10.3390/life10060083.

Behrendt L, Trampe EL, Nord NB, *et al.* Life in the dark: Far-red absorbing cyanobacteria extend photic zones deep into terrestrial caves. *Environ Microbiol* 2020;22(3):952–963; doi: 10.1111/1462-2920.14774.

Billi D, Verseux C, Fagliarone C, *et al.* A desert cyanobacterium under simulated Mars-like conditions in low Earth orbit: Implications for the habitability of Mars. *Astrobiology* 2019; 19(2):158–169; doi: 10.1089/ast.2017.1807.

Blanco Y, Quesada A, Gallardo-Carreño I, *et al.* CYANOCHIP: An antibody microarray for high-taxonomical-resolution cyanobacterial monitoring. *Environ Sci Technol* 2015;49(3): 1611–20; doi: 10.1021/es5051106.

Blanco Y, de Diego-Castilla G, Viúdez-Moreiras D, *et al.* Effects of gamma and electron radiation on the structural integrity of organic molecules and macromolecular biomarkers measured by microarray immunoassays and their astrobiological implications. *Astrobiology* 2018;18(12):1497–1516; doi: 10.1089/ast.2016.1645.

Carr CE, Bryan NC, Saboda KN, *et al.* Nanopore sequencing at Mars, Europa, and microgravity conditions. *npj Microgravity* 2020;6:24; doi: 10.1038/s41526-020-00113-9.

Carrier BL, Abbey WJ, Beegle LW, *et al.* Attenuation of ultraviolet radiation in rocks and minerals: Implications for Mars science. *J Geophys Res Planets* 2019;124(10):2599–2612; doi: 10.1029/2018JE005758.

Cassaro A, Pacelli C, Aureli L, *et al.* Antarctica as a reservoir of planetary analogue environments. *Extremophiles* 2021; 25(5–6):437–458; doi: 10.1007/s00792-021-01245-w.

Cheptsov VS, Vorobyova EA, Osipov GA, *et al.* Microbial activity in martian analog soils after ionizing radiation: Implications for the preservation of subsurface life on Mars. *AIMS Microbiol* 2018;4(3):541–562; doi: 10.3934/microbiol.2018.3.541.

Cheptsov VS, Belov AA, Vorobyova EA, *et al.* Resistance of enzymes to ionizing radiation under model conditions of the martian regolith. *Sol Syst Res* 2021;55:383–388; doi: 10.1134/S003809462104002X.

Cockell CS, Raven JA. Zones of photosynthetic potential on Mars and early Earth. *Icarus* 2004;169(2):300–310.; doi: 10.1016/j.icarus.2003.12.024

Cockell CS, Catling DC, Davis WL, *et al.* The ultraviolet environment of Mars: Biological implications past, present, and future. *Icarus* 2000;146(2):343–59; doi: 10.1006/icar.2000.6393.

Cockell CS, Schuerger AC, Billi D, *et al.* Effects of a simulated martian UV flux on the cyanobacterium, *Chroococcidiopsis* sp. 029. *Astrobiology* 2005;5(2):127–40; doi: 10.1089/ast.2005.5.127.

Cockell CS, Rettberg P, Rabbow E, *et al.* Exposure of phototrophs to 548 days in low Earth orbit: Microbial selection

pressures in outer space and on early Earth. *ISME J* 2011;5: 1671–1682; doi: 10.1038/ismej.2011.46.

Dartnell LR, Desorgher L, Ward JM, *et al.* Modelling the surface and subsurface martian radiation environment: Implications for astrobiology. *Geophys Res Lett* 2007;34(2): L02207; doi: 10.1029/2006GL027494.

Davila AF, Schulze-Makuch D. The last possible outposts for life on Mars. *Astrobiology* 2016;16(2):159–68; doi: 10.1089/ast.2015.1380.

de Diego-Castilla G, Cruz-Gil P, Mateo-Marti E, *et al.* Assessing antibody microarrays for space missions: Effect of long-term storage, gamma radiation, and temperature shifts on printed and fluorescently labeled antibodies. *Astrobiology* 2011;11(8):759–773; doi: 10.1089/ast.2011.0647.

de Vera J-P, Alawi M, Backhaus T, *et al.* Limits of life and the habitability of Mars: The ESA space experiment BIOMEX on the ISS. *Astrobiology* 2019;19(2):145–157; doi: 10.1089/ast.2018.1897.

Ertem G, Ertem MC, McKay CP, *et al.* Shielding biomolecules from effects of radiation by Mars analogue minerals and soils. *Int J Astrobiol* 2017;16(3):280–285; doi: 10.1017/S1473550416000331.

Ertem G, Glavin DP, Volpe RP, *et al.* Evidence for the protection of N-heterocycles from gamma radiation by Mars analogue minerals. *Icarus* 2021;368:114540; doi: 10.1016/j.icarus.2021.114540.

Fagliarone C, Mosca C, Ubaldi I, *et al.* Avoidance of protein oxidation correlates with the desiccation and radiation resistance of hot and cold desert strains of the cyanobacterium *Chroococcidiopsis*. *Extremophiles* 2017;21(6):981–991; doi: 10.1007/s00792-017-0957-8.

Fagliarone C, Napoli A, Chiavarini S, *et al.* Biomarker preservation and survivability under extreme dryness and Mars-like UV flux of a desert cyanobacterium capable of trehalose and sucrose accumulation. *Front Astron Space Sci* 2020;7:31; doi: 10.3389/fspas.2020.00031.

Fairén AG, Gómez-Elvira J, Briones C, *et al.* The Complex Molecules Detector (CMOLD): A fluidic-based instrument suite to search for (bio)chemical complexity on Mars and icy moons. *Astrobiology* 2020;20(9):1076–1096; doi: 10.1089/ast.2019.2167.

Farley KA, Malespin C, Mahaffy P, *et al*. In situ radiometric and exposure age dating of the martian surface. *Science* 2014; 343(6169):1247166; doi: 10.1126/science.1247166.

Friedmann EI, Ocampo R. Endolithic blue-green algae in the Dry Valleys: Primary producers in the Antarctic desert ecosystem. *Science* 1976;193(4259):1247–1249; doi: 10.1126/science.193.4259.124.

Fox AC, Eigenbrode JL, Freeman KH. Radiolysis of macromolecular organic material in Mars-relevant mineral matrices. *J Geophys Res Planets* 2019;124(12):3257–3266; doi: 10.1029/2019JE006072.

García-Descalzo L, Parro V, García-Villadangos M, *et al.* Microbial markers profile in anaerobic Mars analogue environments using the LDChip (Life Detector Chip) antibody microarray core of the SOLID (Signs of Life Detector) platform. *Microorganisms* 2019; 7(9):365; doi: 10.3390/microorganisms7090365.

Gómez-Elvira J, Armiens C, Carrasco I, *et al*. Curiosity's rover environmental monitoring station: Overview of the first 100 sols. *J Geophys Res Planets* 2014;119:1680–1688; doi: 10.1002/2013JE004576.

Hassler DM, Zeitlin C, Wimmer-Schweingruber RF, *et al.* Mars' surface radiation environment measured with the Mars Science Laboratory's Curiosity rover. *Science* 2014; 343(6169):1244797; doi: 10.1126/science.1244797.

Maggiori C, Stromberg J, Blanco Y, *et al.* The limits, capabilities, and potential for life detection with MinION sequencing in a paleochannel Mars analog. *Astrobiology* 2020;20(3):375–393; doi: 10.1089/ast.2018.1964.

Marshall CP, Edwards HG, Jehlicka J. Understanding the application of Raman spectroscopy to the detection of traces of life. *Astrobiology* 2010;10(3):229–43; http://doi.org/10.1089/ast.2009.0344.

Martins Z. Detection of organic matter and biosignatures in space missions. *Curr Issues Mol Biol* 2020;38:53–74; doi: 10.21775/cimb.038.053.

Martins Z, Cottin H, Kotler JM, *et al.* Earth as a tool for astrobiology—a European perspective. *Space Sci Rev* 2017; 209:43–81; doi: 10.1007/s11214-017-0369-1.

McKay CP, Stoker C, Glass B, *et al.* The Icebeaker life mission to Mars: A search for biomolecular evidence for life. *Astrobiology* 2013;13(4):334–53; doi: 10.1089/ast.2012.0878.

Megevand V, Viennet JC, Balan E, *et al.* Impact of UV radiation on the Raman signal of cystine: Implications for the detection of S-rich organics on Mars. *Astrobiology* 2021; 21(5):566–574; doi: 10.1089/ast.2020.2340.

Mosca C, Napoli A, Fagliarone C, *et al.* Role of DNA repair pathways in the recovery of a dried, radioresistant cyanobacterium exposed to high-LET radiation: Implications for the habitability of Mars. *Int J Astrobiol* 2022;1–12; doi: 10.1017/S1473550422000131.

Parro V, de Diego-Castilla G, Rodríguez-Manfredi, *et al.* SOLID3: a multiplex antibody microarray-based optical sensor instrument for in situ life detection in planetary exploration. *Astrobiology* 2011;11(1):15–28; doi: 10.1089/ast.2010.0501.

Rivas LA, García-Villadangos M, Moreno-Paz M, *et al.* A 200-antibody microarray biochip for environmental monitoring: searching for universal microbial biomarkers through immunoprofiling. *Anal Chem* 2008;80(21):7970–7979; doi: 10.1021/ac8008093.

Rojas Vivas JA, Navarro-González R, de la Rosa J, *et al.* Radiolytic degradation of soil carbon from the Mojave Desert by ^{60}Co gamma rays: Implications for the survival of martian organic compounds due to cosmic radiation. *Astrobiology* 2021;21(4):381–393; doi: 10.1089/ast.2020.2257.

Rull F, Maurice S, Hutchinson I, *et al.* The Raman laser spectrometer for the ExoMars rover mission to Mars. *Astrobiology* 2017;17(7):627–654; doi: 10.1089/ast.2016.1567.

Sánchez-García L, Fernández-Martínez MÁ, Moreno-Paz M, *et al.* Simulating Mars drilling mission for searching for life: *Ground-truthing* lipids and other complex microbial biomarkers in the iron-sulfur rich Río Tinto analog. *Astrobiology* 2020;20(9):1029–1047; doi: 10.1089/ast.2019.2101.

Smith HD, Baqué M, Duncan AG, *et al.* Comparative analysis of cyanobacteria inhabiting rocks with different light transmittance in the Mojave Desert: A Mars terrestrial analogue. *Int J Astrobiol* 2014;13(3):271–277; doi: 10.1017/S1473550414000056.

Sunshine D. Mars science laboratory CHIMRA: A device for processing powdered martian samples. In *Proceedings of the 40th Aerospace Mechanisms Symposium.* Kennedy Space Center, Cocoa Beach, FL, 2010; NTRS Document ID 20100021925.

Vago JL, Westall F, Coates AJ, *et al.* Habitability on early Mars and the search for biosignatures with the ExoMars rover. *Astrobiology* 2017;17(6–7):471–510; doi: 10.1089/ast.2016.1533.

Verseux C, Baqué M, Cifariello R, *et al.* Evaluation of the resistance of *Chroococcidiopsis* spp. to sparsely and densely ionizing irradiation. *Astrobiology* 2017;17(2):118–125; doi: 10.1089/ast.2015.1450.

Westall F, Foucher F, Bost N, *et al.* Biosignatures on Mars: What, where, and how? Implications for the search for martian life. *Astrobiology* 2015;15(11):998–1029; doi: 10.1089/ast.2015.1374.

Wiens RC, Maurice S, Robinson SH, *et al.* The SuperCam instrument suite on the NASA Mars 2020 rover: Body unit and combined system tests. *Space Sci Rev* 2021;217:4; doi: 10.1007/s11214-020-00777-5.

Address correspondence to:
Daniela Billi
Department of Biology
University of Rome Tor Vergata
Via della Ricerca Scientifica
Rome 00133
Italy

E-mail: billi@uniroma2.it

Submitted 20 January 2022
Accepted 20 June 2022

Associate Editor: Don Cowan

Abbreviations Used

BIOMEX = Biology and Mars Experiment
CCMEE = Culture Collection of Microorganisms from Extreme Environments
FSMI = fluorescent sandwich microarray immunoassay
P-MRS = Phyllosilicatic Mars Regolith Simulant
S-MRS = Sulfatic Mars Regolith Simulant
SOLID = Signs of Life Detector